Derivation of the stress concentrations at holes in orthotropic plates using thermoelastic stress analysis

S. Quinn, S. Sambasivam and J.M. Dulieu-Barton
School of Engineering Sciences, University of Southampton, Highfield, Southampton SO17 1BJ, United Kingdom

Abstract

An experimental study of the stress distribution around holes in orthotropic composite laminates has been conducted using thermoelastic stress analysis (TSA). Quantitative thermoelastic studies of stress concentrations in metallic plates is a straightforward matter, all that is required is the ratio of the response from the hole and a far-field reading. For orthotropic materials the situation is more complex as the response is not simply proportional to the sum of the principal stresses. In general the thermoelastic response of an orthotropic laminate is a function of the stresses in the principal surface material directions and the associated coefficient of thermal expansion. The approach in this paper is to obtain 'stress factors' at the hole and identify the maxima in the plot. Specimens manufactured from a variety of different laminate lay-ups (unidirectional (UD), cross-ply (CP), angle-ply (AP) and quasi-isotropic (QI)) are considered. In all these cases the principal stress directions at the hole are not coincident with the principal material directions and it is a challenging proposition to derive meaningful stress data from these configurations. To validate the approach the experimental data are compared to analytical models. To better understand the nature of the response finite element models are produced that mimic the thermoelastic response.

Introduction

Composite components with holes or cut-outs of various sizes and shapes are frequently used as load bearing members in various engineering structures. The presence of stress concentrators causes substantial perturbation of the stress and strain field in the structure under service loads. Therefore it is of great practical interest to accurately analyse the load bearing capacity of these structures. Numerous numerical studies [1-4] on anisotropic composite plates with holes of various geometries, lay-ups and loading conditions have been conducted. The heterogeneity and directional anisotropy of composite plates complicates the mathematical formulation of the stress concentration factor (SCF) around holes. A theoretical solution to obtain SCF's in an infinite orthotropic plate for both circular and elliptical holes under tensile load using the complex variable method was presented by Lekhnitskii [5]. In addition, several experimental techniques such as digital image correlation (DIC) [6], Moiré methods [7], thermoelastic stress analysis (TSA) [8] and strain gauging [9] have been used to determine the strain/stress distribution around circular holes in orthotropic plates. Some experimental and theoretical results that attempt to incorporate a finite width correction factor around the hole are presented in Ref. [9], which is important in the interpolation of test data to infinite plate results.

The TSA technique is based on infra-red thermography, where the small temperature changes resulting from a change in elastic stress are obtained by measuring the change in infra-red photon emission. TSA has advantages over other experimental techniques since only minimal surface preparation (i.e. coatings, grids or speckle patterns are not needed) is required for obtaining stress data with spatial resolution down to 4 μm [10]. The purpose of this paper is to obtain the stress/strain concentration at holes in orthotropic polymer composite plates from thermoelastic data. To achieve this it is necessary to understand the

nature of the thermoelastic response; three approaches are presented for interpreting the thermoelastic data. A variety of lay-ups are studied and analytical and finite element models are used to aid the interpretation of the TSA data. To achieve accurate insight from the models the material properties required to present the data in the same form as the TSA are derived experimentally for the different material configurations. The results show that the thermoelastic response is most similar to the 'global' response of the laminate and not that of the surface ply or resin rich layer.

Derivation of the thermoelastic stress and strain concentration factors

A stress concentration factor, SCF_σ, for a single hole in the centre of a strip of material loaded under uniform uniaxial loading is defined as follows:

$$SCF_\sigma = \frac{\sigma_{Hole}}{\sigma_{Far-field}} \quad (1)$$

where σ is the principal stress.

Figure 1 shows a strip of orthotropic material with a central circular hole loaded along the principal axes (Figure 1a) and loaded 'off axis' (Figure 1b). To relate the stresses at the hole to those in the plate it is simpler to define the stresses at the hole in a polar coordinate system and the stresses in the far-field in a Cartesian system, as shown in Figure 1. In the polar coordinate system the laminate stresses are defined as: σ_{rL} (radial stress), $\sigma_{\theta L}$ (tangential stress) and $\sigma_{r\theta L}$ (shear stress). At the edge of hole the radial stress and shearing stress are both zero, since no external tractions exist at the periphery of the hole.

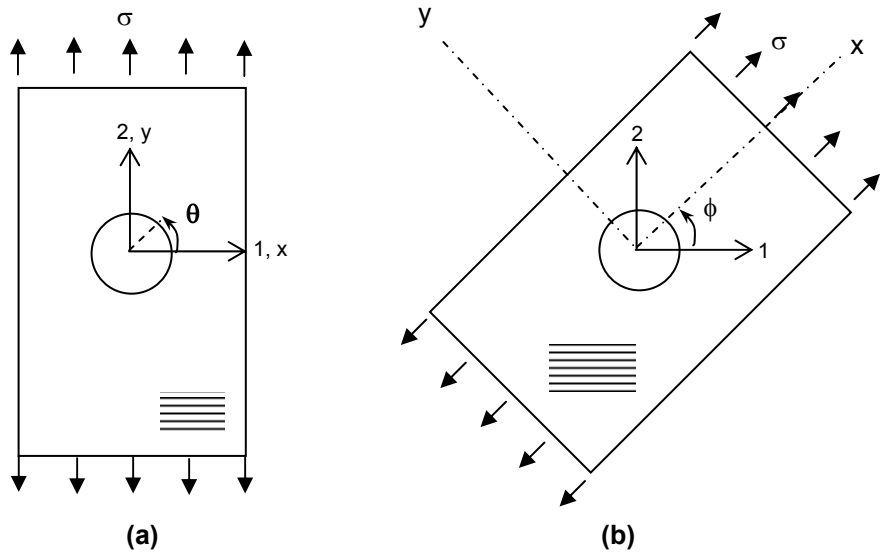

Figure 1: Uniaxial tensile load applied a) in the principal directions and b) at an angle to the principal material direction of an orthotropic plate with a circular hole

Also, to satisfy the stress free boundary condition in the far-field, when taking the laminate as a homogeneous body, only the applied stress exists so the SCF_σ is generally given as:

$$SCF_\sigma = \frac{\sigma_{\theta L}}{\sigma_{app}} \tag{2}$$

where $\sigma_{\theta L}$ is the laminate tangential stress at the hole and σ_{app} is the stress applied to the laminate.

The thermoelastic temperature change, ΔT, for a composite lamina (e.g. the surface ply of a composite laminate) is given by [11]:

$$\begin{aligned}\Delta T &= -\frac{T}{\rho C_p}\left(\alpha_x\sigma_x + \alpha_y\sigma_y + \alpha_{xy}\sigma_{xy}\right)\\ &= -\frac{T}{\rho C_p}\left(\alpha_1\sigma_1 + \alpha_2\sigma_2 + \alpha_{12}\sigma_{12}\right)\\ &= -\frac{T}{\rho C_p}\left(\alpha_r\sigma_r + \alpha_\theta\sigma_\theta + \alpha_{r\theta}\sigma_{r\theta}\right)\end{aligned} \tag{3}$$

where T is the surface temperature, ρ is the density, C_p is the specific heat at constant pressure, α is the coefficients of thermal expansion (CTE) and the subscripts x,y denote the principal stress direction in the surface ply, 1,2 are in the principal material directions of the surface ply and r,θ denotes the system in the surface ply in polar coordinates.

It is important to note that the bracketed term in Equation (3) is an invariant since ΔT is a scalar quantity [12]. Equation (3) deals with the surface ply. In this case the shear terms in the xy direction disappear as σ_{xy} is zero in the principal stress directions and the shear terms in the 12 direction also disappear as α_{12} is zero in the principal material directions. It is only in the last expression in Equation (3) that the shear terms need to be retained. Even if the values are taken at the hole for a general laminate both the radial and shear stresses will exist. Equation (3) could be recast to denote the overall behaviour of the laminate, treating it as an orthotropic homogeneous block of material. Here the shear terms in the first and second expressions vanish to zero as before. In the third expression in Equation (3) the laminate radial stress and shear stress would also be zero.

It is possible to formulate the stress concentration factor from TSA data (SCF_{TSA}) in three different ways [12]. Firstly, and most conventionally, it is assumed that the thermoelastic response is purely from the surface ply, so that:

$$\frac{\Delta T_H}{\Delta T_F} = \frac{\alpha_r\sigma_r + \alpha_\theta\sigma_\theta + \alpha_{r\theta}\sigma_{r\theta}}{\alpha_1\sigma_1 + \alpha_2\sigma_2} \tag{4}$$

where σ_1 and σ_2 are the stress changes in the principal material directions ($\alpha_{12} = 0$) and ΔT_H and ΔT_F are the measured thermoelastic temperature changes at the hole and in the far field-region, respectively.

The second option is to define the thermoelastic response as a function of the global laminate behaviour to correspond best with the definition given by Equation (1) so that SCF_{TSA} is defined as:

$$\frac{\Delta T_H}{\Delta T_F} = \frac{\alpha_{\theta L}\sigma_{\theta L}}{\alpha_{1L}\sigma_{1L}} \tag{5}$$

where the subscript L denotes the laminate behaviour.

For laminated composites with a low thermal conductivity (e.g. GFRP) under adiabatic conditions, the thermoelastic effect from the inner zones of the material is not able to affect the surface temperature.

Therefore, the measured thermoelastic temperature change relies on the properties of the surface material. In Ref. [13] it was shown that the presence of the surface resin layer on a composite laminate can replicate the strain field of the laminate and serves as a strain witness in GFRP composites, which provides the third case for comparison, where the thermoelastic temperature change can be expressed as follows:

$$\Delta T = -\frac{\alpha_m T}{\rho_m C_{Pm}}\left[\frac{E_r}{1-\nu_m}(\varepsilon_{xc}+\varepsilon_{yc})\right] \tag{6}$$

where the subscripts m and c signify the properties of the resin and the composite respectively.

For the treatment in Equation (6), it is more appropriate to consider a strain concentration factor, SCF_ε, that can be defined as follows:

$$SCF_\varepsilon = \frac{\varepsilon_\theta}{\varepsilon_{app}} \tag{7}$$

where ε_θ and ε_{app} denote the local strain and applied strain, respectively.

The SCF_ε is generally not equal to SCF_σ because of the difference in the directional modulus of the laminate, i.e.:

$$SCF_\varepsilon = \frac{\varepsilon_\theta(\theta=0)}{\varepsilon_{app}} = \frac{a_\theta \sigma_\theta(\theta=0)}{a_L \sigma_{app}} = \frac{a_\theta}{a_L} SCF_\sigma \tag{8}$$

where a_θ and a_L are the compliances of the laminate. Therefore, SCF_σ is only equal to SCF_ε when $a_\theta = a_L$.

Since the resin layer is isotropic, SCF_ε is equal to SCF_σ, then a third formulation of the SCF_{TSA} is as follows:

$$\frac{\Delta T_H}{\Delta T_F} = \frac{\varepsilon_\theta}{(\varepsilon_{xc}+\varepsilon_{yc})} \tag{9}$$

Thermoelastic stress analysis of holes in laminated composites

Four different glass/epoxy laminate panels with different ply orientations (i.e. UD, CP, QI, and AP) were manufactured for the experimental study. All the laminates have a 0^o surface ply, except for the AP. The material used for manufacturing the test specimens was a unidirectional glass/epoxy pre impregnated (E-glass and Novalac epoxy resin) material supplied by Primco Limited. The fibre volume fraction was approximately 52%. The specimens were manufactured by curing for 1 hour at 125°C under 3 bar of pressure in an autoclave and post curing at 150°C for 16 hours. Specimens containing a central circular hole were machined from the composite panels. All the specimens had a 10 mm central circular hole produced with a tungsten carbide drill to minimise machining damage. The dimensions of the specimens and the loading conditions are given in Table 1. To minimise the effect of signal noise, the applied loads for the TSA tests were chosen to give a strong thermoelastic response from each laminate; the effect of the mean load on the thermoelastic signal has previously been shown not to be significant [12].

A Silver 480M infra-red system from FLIR systems (formerly known as CEDIP Infrared Systems), comprising a high performance InSb focal plane array detector, was used to collect the TSA data. The system is radiometrically calibrated, so the infra-red data can be outputted or converted to ΔT values directly. The specimens were unpainted as epoxy has a naturally high surface emissivity. A loading frequency of 10 Hz was used as previous work [12] indicated that this was sufficient to achieve adiabatic

conditions for these materials. TSA data around the hole and the far-field region was collected from all four specimens.

The TSA will provide directly the quantities in the left hand side of Equations (4), (5), (6) and (9). To populate the right hand side of these equations and combine with the stresses obtained from the analytical and finite element models (described in the next section) it was necessary to obtain the material properties of the specimens. The in-plane mechanical properties of the epoxy and composite materials were measured according to ASTM D638-03 [14] and these are given in Table 2 and Table 3 for the epoxy, lamina (i.e. surface ply) and laminates respectively. The physical properties such as density, specific heat capacity and coefficient of thermal expansion (CTE) were determined according to appropriate standards [15, 16] and these are also given in Table 2 for the epoxy resin and the UD laminate.

Table 1: Applied loading conditions for the specimens with a hole

Specimen	**Stacking sequence**	**Dimensions (mm)**			**Applied load (kN)**	
		Length	**Width**	**Thickness**	**Mean load**	**Amplitude**
UD	$[0]_6$	251.0	39.3	1.50	3.0	1.0
CP	$[0,90]_s$	249.2	40.8	1.00	2.0	1.0
QI	$[0,\pm45,90]_s$	249.1	39.8	1.90	3.0	1.0
AP	$[\pm45]_s$	249.7	38.5	1.00	0.6	0.5

Table 2: Mechanical and physical properties of the lamina and the epoxy resin

Specimen	**Young's Modulus (GPa)**		**Poisson's ratio**		**Density, ρ (kg/m^3)**	**CTE, ($x10^{-6}$/°C)**		**C_p, (J/(kg°C))**
	E_1	**E_2**	**ν_{12}**	**ν_{21}**		**α_1**	**α_2**	
UD (lamina)	34.2	10	0.33	0.10	1230	9.0	31.0	843
Epoxy	4.2	n/a	0.41	n/a	1207	52.0	n/a	1230

Table 3: Global mechanical and physical properties of the CP, AP and QI laminates

Specimen	**Young's modulus, E_{1L} (GPa)**	**Poisson's ratio, ν_{12L}**	**CTE, α_{1L} (x 10^{-6}/°C)**
CP	20.0	0.15	10.59
AP	9.5	0.55	16.20
QI	20.0	0.29	9.25

Analytical model and finite element analysis of composite laminates with holes

The analytical solution for the stress distribution in an orthotropic plate with a circular opening is [5]:

$$SCF_{\sigma} = \frac{\sigma_{\theta}}{\sigma_{app}} = \frac{E_{\theta}}{E_1}\left[-\cos^2\phi + (k+n)\sin^2\phi\right]k\cos^2\theta + [(1+n)\cos^2\phi - k\sin^2\phi]\sin^2\theta$$
$$-n(1+k+n)\sin\phi\cos\phi\sin\theta\cos\theta \qquad (10)$$

where E_{θ} is the Young's modulus in the θ direction, (see Figure 1), and n and k are constants based on material properties. It is also worth noting that the size of the hole is not accounted for in this solution. This equation can be modified according to Equation (6) to provide SCF_{TSA} values.

To aid the interpretation of the TSA data, Finite Element (FE) models of the specimens were produced using ANSYS commercial software. The 2D finite element model was developed using 8-node structural solid elements (PLANE82). A series of rectangular plates with the same geometry and loading conditions as the specimens tested in the experimental programme have been modelled for the different laminate types. Due to the symmetric nature of the specimen, only quarter models have been considered, see Figure 2. The material properties assigned to the laminate were the same as in Tables 2 and 3. A denser mesh was used close to the hole to capture the stress gradient accurately, as shown in Figure 3. The equivalent SCF_{TSA} values for the orthotropic plates were calculated using Equations (4), (5) and (9) from the raw FE output (i.e. stress and strain values) using the measured CTE values. To evaluate SCF_{TSA} based on Equation (4) the 2D model (known as 2D_4) for the surface ply only (i.e. the UD surface layer for the UD, CP, and QI models and the AP surface layer for the AP model) is modelled for a given applied load. For Equations (5) and (9) the stress and strain have been evaluated for the laminate as a whole.

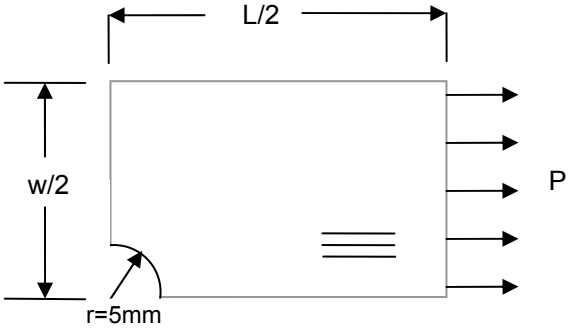

Figure 2: Orthotropic plate with a central circular under uniaxial tension in the x-axis (quarter FE model)

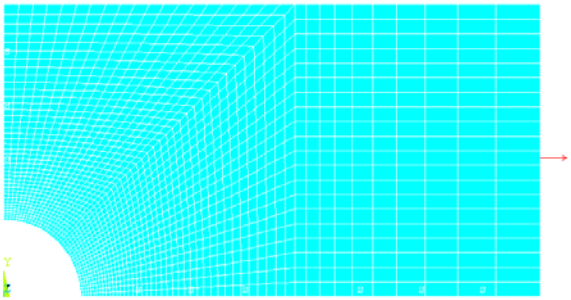

Figure 3: Typical FE model mesh of the composite laminates

Results and Discussion

The values of the maximum SCF_{TSA} values for the experimental, analytical and FEA data and the position around the hole are shown for the different lay-ups in Table 4. By comparing the values of the maximum SCF_{TSA} it is difficult to identify a clear match between the experimental data using any of the treatments derived above. It is the case that in the presence of large stress gradients, such as those experienced local to the holes, non-adiabatic behaviour may occur. To investigate if the large mismatch in the derived SCF_{TSA} values could be attributed to non-adiabatic effects, values of SCF_{TSA} were obtained around the hole, away from the maxima, in increments of 10 degrees. These were compared with the values obtained from the FEA and analytical model for the three different treatments. The SCF_{TSA} data presented in Figures 4 to Figure 7 are shown for a quarter of the region around the hole (i.e. from 0 to 90°). The most striking feature is that only for the QI plate is there any correspondence in data at the 0° position. In all cases the agreement improves away from this region, indicating that non-adiabatic effects could be the cause of the poor agreement in the SCF_{TSA} values given in Table 4. It is clear from all the figures that the strain witness surface resin layer response approach given by Equation (9) shows the greatest deviation from the experimental data in all cases, which indicates that the strain witness assumption is not valid in this application. The analytical model (analytical_5) and FEA model (FEA_5) are in close agreement with each other and with the experimental data. This indicates that the thermoelastic response is a function of the global laminate behaviour and not that of the surface ply. In general, it can be concluded that the FEA_5 assumption gives the best agreement to the experimental data. This is exemplified for the QI laminate with very clear correlation between the experimental data and the analytical and FE model. It is also important to note that the 2D finite element model (i.e. FEA_4) neglects the influence from the adjacent plies. Therefore, there is a requirement for a 3D FE model to better simulate the ply-by-ply material behaviour and this will be the object of future work.

Table 4: Values and position of the maximum SCF_{TSA} for the different composite laminates

Specimen	Experimental		Analytical (Equation 5)		FEA (Equation 4)		FEA (Equation 5)		FEA (Equation 9)	
	SCF_{TSA}	Position, θ (°)	SCF_{TSA}	θ (°)	SCF_{TSA}	θ (°)	SCF_{TSA}	θ (°)	SCF_{TSA}	θ (°)
UD	3.83	0	5.21	0	4.57	0	5.19	0	5.23	0
CP	2.81	170	4.04	0	4.56	0	4.18	0	5.91	0
QI	3.38	180	2.93	0	4.52	0	3.14	0	5.04	0
AP	3.80	0	2.56	25	3.91	34	2.73	0	5.08	0

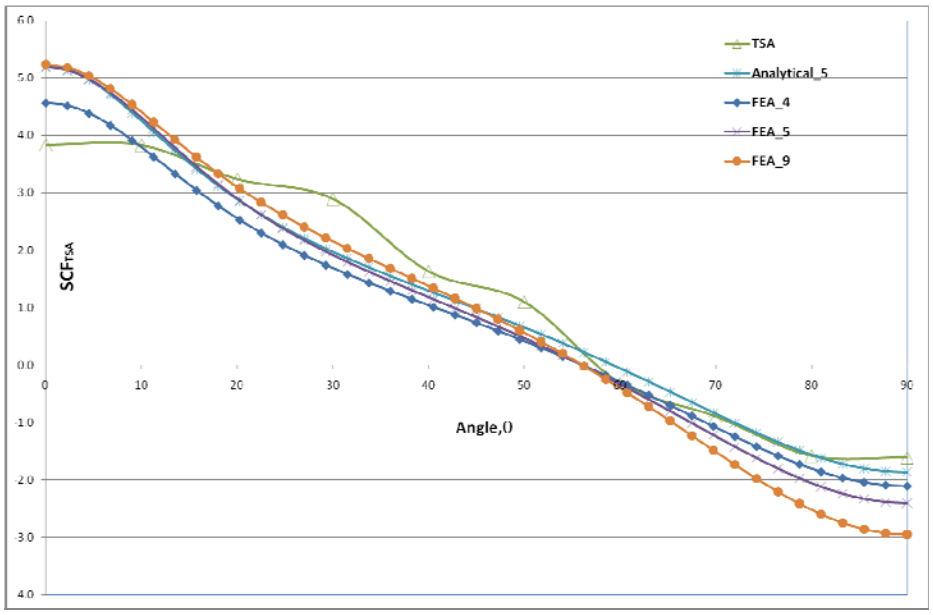

Figure 4: Comparison of experimental SCF_{TSA} with those from an analytical solution and FEA for a UD laminate with a central circular hole

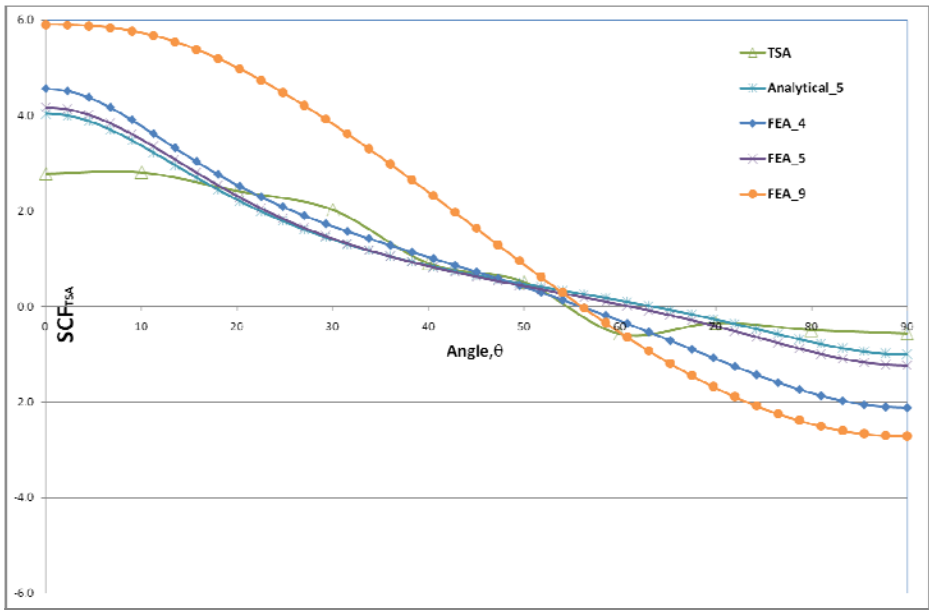

Figure 5: Comparison of experimental SCF_{TSA} with those from an analytical solution and FEA for a CP laminate with a central circular hole

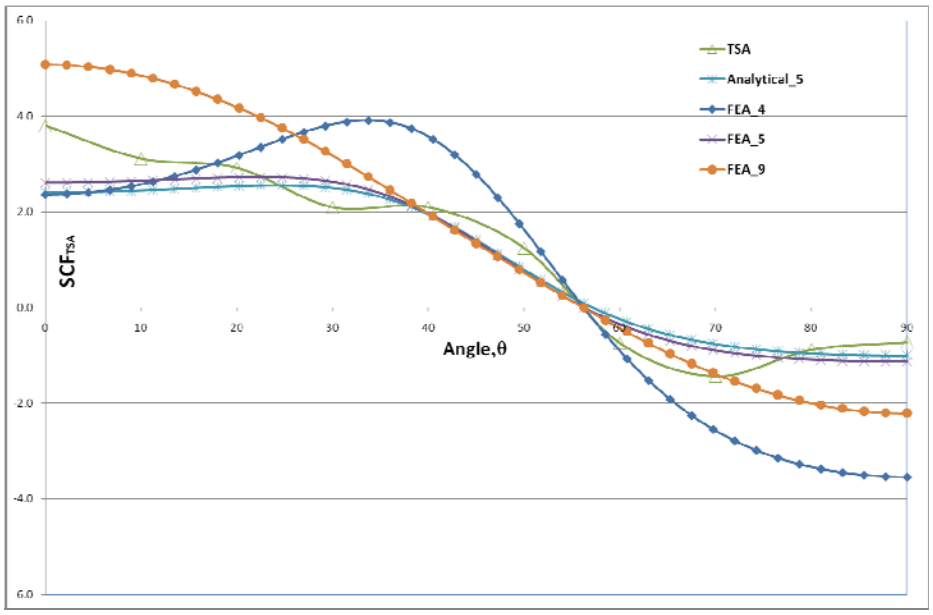

Figure 6: Comparison of experimental SCF_{TSA} with those from an analytical solution and FEA for an AP laminate with a central circular hole

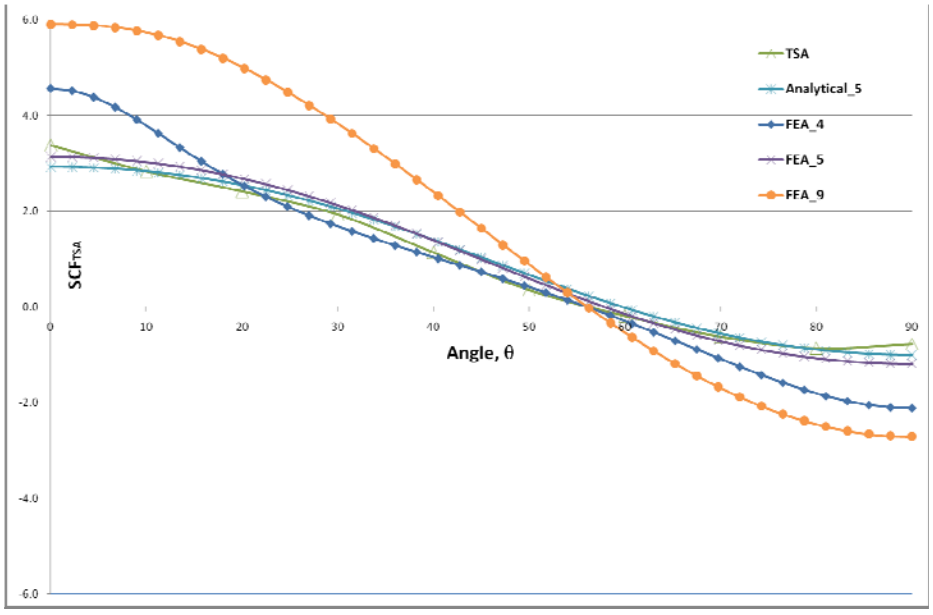

Figure 7: Comparison of experimental SCF_{TSA} with those from an analytical solution and FEA for a QI laminate with a central circular hole

Closure

The paper describes a novel attempt to examine different approaches in quantifying the thermoelastic response from the neighbourhood of holes in orthotropic composite laminates as an 'SCF_{TSA}'. The different approaches are compared with analytical and finite element models. The results show that the SCF_{TSA} derived for composite materials is influenced by global laminate properties. The assumption that the thermoelastic response depends solely on the properties of the surface layer (i.e. the resin rich layer or the orthotropic surface ply) of composite laminates is not compelling and further work to assess the independent behaviour of different lay-ups and their influence on the thermoelastic response is required.

References

[1] Konish, H.J. and Whitney, J.M., "Approximate Stresses in an Orthotropic Plate Containing a Circular Hole", Journal of Composite Materials, 9, 157-166, 1975

[2] Tan, S.C., "Laminated Composite Containing an Elliptical opening I. Approximate Stress Analyses and Fracture Models", Journal of Composite Materials, 21, 925-948, 1987

[3] Whitney, J.M. and Nuismer, R.J., "Uniaxial Failure of Composite Laminates Containing Stress concentrations", Fracture Mechanics of Composites, ASTM STP 593,117-142, 1975

[4] Awerbuch, J. and Madhukar, M., "Notched Strength of Composite Laminates: Predictions and Experiments-A Review", Journal of Reinforced Plastics and Composites, 4, 3-159, 1985

[5] Lekhnitskii, S.G., "Theory of Elasticity of an Anisotropic Elastic Body", Gordon and Breach Science Publishers, 1967

[6] Lotfi, T., K. Moussa, and B. Lorrain, "Stress concentration in a circular hole in a composite plate", Composite structures, 68, 31–36, 2005

[7] Chern, S.M. and Tuttle, M.E., (eds.), "Displacement Fields around a Circular Hole in Composite Laminates", Recent Advances in Experimental Mechanics, Springer, 701-712, 2004

[8] Feng, Z., et al., "Thermoelastic determination of individual stress components in loaded composites", Experimental Mechanics, 32, 85-95, 1992

[9] Tan, S.C.,"Stress Concentration in Laminated Composites", Lancaster:Technomic,1994

[10] Bremond, P., "New developments in Thermoelastic Stress Analysis by Infrared Thermography", IV Pan-American conference for non-destructive testing, Buenos Aires, 2007

[11] Stanley, P. and W.K. Chan, "The application of thermoelastic stress analysis techniques to composite materials", Journal of Strain Analysis, 23, 137-143, 1988

[12] Sambasivam, S., Quinn, S. and Dulieu-Barton, J.M. "Identification of the source of the thermoelastic response from the orthotropic laminated composites", Accepted for publication at the 17th International Conference on Composite Materials, Edinburgh, UK, July 2009

[13] Emery, T.R., Dulieu-Barton, J.M., Earl, J.S. and Cunningham, P.R., "A generalised approach to the calibration of orthotropic materials for thermoelastic stress analysis", Composites Science and Technology, 68, 743-752, 2008

[14] ASTM D638-03, Standard test method for tensile properties of plastics

[15] Lanza di Scalea, F., "Measurement of Thermal Expansion Coefficients of composites Using Strain Gages", Experimental Mechanics, 38, 233-241, 1998

[16] ISO 11357, Plastics - Differential scanning calorimetry (DSC) - Part 4: Determination of specific heat capacity